

磁场作用功能梯度壳体磁弹耦合动力学模型^{*}

胡宇达^{1,2}, 廖峰^{1,2}

(1. 燕山大学 建筑工程与力学学院, 河北 秦皇岛 066004;

2. 燕山大学 河北省重型装备与大型结构力学可靠性重点实验室, 河北 秦皇岛 066004)

摘要: 针对电磁场环境中金属-陶瓷功能梯度圆柱壳体结构, 基于物理中面下的几何关系和 Hooke 定律, 确定了圆柱薄壳体的非线性本构关系. 根据 Kirchhoff-Love 弹性理论, 给出了非均质弹性壳体的变形应变能、动能及其变分运算式. 基于电磁弹性理论, 得出了电磁场作用下磁性功能梯度壳体所受涡流 Lorentz 力和磁化力模型. 应用 Hamilton 广义变分原理, 建立功能梯度薄壳体的磁弹性耦合非线性振动方程组, 得出了描述功能梯度结构的具有变形场与电磁场耦合特征的动力学理论模型. 通过对磁场中功能梯度壳体固有振动问题的举例分析, 得到了壳体振动特征方程和固有频率变化规律, 表明磁场和材料体积分数指数的增大能够使频率值减小, 而在周向波数影响曲线中出现频率最小值的情形. 研究方法可为多场耦合系统理论建模及动力学分析提供参考.

关键词: 功能梯度圆柱壳; 磁弹性; 动力学模型; 电磁场; Hamilton 变分原理

中图分类号: O322; O343.7 **文献标志码:** A **DOI:** 10.21656/1000-0887.440048

A Magnetoelastic Coupling Dynamical Model for Functional Gradient Shells Under Magnetic Field Actions

HU Yuda^{1,2}, LIAO Feng^{1,2}

(1. School of Civil Engineering and Mechanics, Yanshan University,

Qinhuangdao, Hebei 066004, P.R.China;

2. Hebei Key Laboratory of Mechanical Reliability for Heavy Equipment and Large Structures,

Yanshan University, Qinhuangdao, Hebei 066004, P.R.China)

Abstract: For metal-ceramic functional gradient cylindrical shells in electromagnetic fields, the nonlinear constitutive relations were determined based on the geometry and Hooke's law on the physical neutral surface. According to the Kirchhoff-Love theory, the strain energy expression and the kinetic energy expression with its variational operator were given for the heterogeneous elastic shell. The model of the eddy current Lorentz force and the magnetization force for ferromagnetic functional gradient shells under electromagnetic field actions, was derived with the electromagnetic elasticity theory. The magnetoelastic coupling nonlinear vibration equations for the shell were obtained by means of Hamilton's variational principle, and the dynamical model describing the coupling characteristics of the deformation field and the electromagnetic field was established for functional gradient structures. Through numerical examples for natural vibrations of functional gradient shells, the characteristic equation and the natural frequency variation law were obtained. The results show that, the natural

* 收稿日期: 2023-02-27; 修订日期: 2023-05-24

基金项目: 国家自然科学基金项目(12172321); 河北省自然科学基金项目(A2020203007)

作者简介: 胡宇达(1968—), 男, 教授, 博士, 博士生导师(通讯作者. E-mail: huyuda03@163.com).

引用格式: 胡宇达, 廖峰. 磁场作用功能梯度壳体磁弹耦合动力学模型[J]. 应用数学和力学, 2023, 44(11): 1341-1353.

frequency decreases with the magnetic induction intensity and the material volume fraction index, and the phenomenon of minimum frequency will occur in the circumferential wave number influence curves. This study provides a reference for the theoretical modeling and dynamic analysis of multi-field coupling systems.

Key words: functional gradient cylindrical shell; magnetoelasticity; dynamical model; electromagnetic field; Hamilton's variational principle

0 引 言

功能梯度材料(FGM)是指通过结构和组成要素的连续或准连续变化,使材料的性能在空间位置上呈梯度变化的新型非均质复合材料.该材料的显著特点是内部结构材料组分呈连续平滑变化,不存在明显界面,从而能够较好地避免应力集中现象^[1].金属/陶瓷 FGM 是最典型也是最早被研制的 FGM,该材料能够充分发挥陶瓷的耐高温、抗腐蚀和金属的强度高、韧性好等优点,特别在多物理场环境中更能发挥材料性能的梯变优势,值得深入揭示其复杂的力学特性.板壳结构作为 FGM 的常见结构形式,吸引人们开展了许多理论研究.在结构弯曲问题研究中,Yang 等^[2]和 Liu 等^[3]研究了 FGM 圆板轴对称弯曲以及各向同性 FGM 圆板三维弹性问题;Yousefitabar 等^[4]研究了温度载荷作用下 FGM 环板的稳定性及临界屈曲问题;Trabelsi 等^[5]分析了几何和物理参数对 FGM 壳体后屈曲特性的影响;Chan 等^[6]研究了加筋 FGM 圆锥壳体的屈曲和后屈曲问题.在功能梯度结构动力学性能研究中,曹志远^[7]和 Tu 等^[8]基于高阶剪切变形理论研究了 FGM 矩形板固有振动和热弹自由振动问题;Hu 等^[9]研究了热环境中金属/陶瓷 FGM 圆板非线性共振及分岔特性;Zhang 等^[10]和 An 等^[11]分别研究了 FGM 圆柱壳和截锥壳的非线性动力学及混沌问题;Sahu 等^[12]分析了双弯曲黏弹性金属/陶瓷 FGM 夹层壳结构固有振动特性;Li 等^[13]研究了热环境中旋转 FGM 圆柱壳参数共振问题;Zhang 等^[14-16]通过引入物理中曲面研究了 FGM 梁、板、壳的非线性动力学问题.电磁弹性理论可以研究弹性介质在电磁场环境中产生变形时力、电、磁等多场量间的相互作用关系.在磁弹性弯曲与振动问题研究中,Miya 等^[17]对处于磁场中铁磁梁板结构屈曲问题开展了研究;刘旭等^[18]研究了热环境旋转功能梯度纳米环板的自由振动问题;陈明飞等^[19]分析了功能梯度三角板的面内振动问题;Wang 等^[20]和 Mohajerani 等^[21]分别研究了磁场中铁磁板的稳定性和振动问题;胡宇达等^[22-24]建立了外加磁场环境中轴向运动导电、导磁薄板的磁固耦合动力学理论模型;沈璐璐和杨博等^[25]研究了功能梯度压电板受均布载荷作用下柱面弯曲问题的弹性应力解;Mikilyana 等^[26]和 Molchenko 等^[27]分别研究了导电壳体结构的磁弹性动力稳定性和变形问题.另外,在功能梯度结构电磁问题研究中,Li 等^[28]针对 FGM 多孔板电磁热弹性振动问题进行了研究;Mehditabar 等^[29]研究了 FGM 圆柱壳的磁热弹弯曲问题.Liu 等^[30]分析了含孔隙率功能梯度压电壳体的力-电-热耦合共振特性.通过上述文献调研可见,关于 FGM 结构动力学研究主要分为两个方向:一是研究形状、尺寸、孔隙等结构自身特性对系统响应的影响;另一方向是探究复杂物理场环境(如热场、电磁场、机械场等)中的动力学问题.目前对于 FGM 结构在电磁场环境下的研究主要集中在压电结构领域,其磁场主要作为电场的伴生场发挥作用.然而,对于导磁、导电 FGM 结构在外加磁场环境下的研究却鲜有报道.事实上,结构在磁场环境下的磁弹耦合更能体现介质与物理场之间的相互“力”效应,一方面,结构受涡流电磁力作用产生变形;另一方面,结构变形影响磁场空间分布形式,使电磁力大小发生改变.这类磁场与结构之间的相互作用常体现为非线性耦合特征,其最终作用效果将直接影响设备服役过程中的安全性和稳定性.对于磁场环境下 FGM 结构的磁弹耦合动力学问题,由于理论建模复杂,数学求解难度大,尚有许多问题需要进一步探索和完善.本文以金属-陶瓷功能梯度壳体结构为对象,开展电磁场作用下多场耦合系统理论建模研究;考虑材料梯度分布规律下的非线性本构关系和电磁影响因素,确定壳体能量关系式和电磁力表征模型;根据能量变分原理和电磁场理论,推导出 FGM 薄壳体的磁弹耦合非线性动力学方程,表征多场量相互作用的耦合机制,并给出壳体固有振动特性的算例结果分析.与以往研究相比,本文的创新性为:① 考虑了介质电导率和磁导率沿厚度方向的梯度变化特征;② 系统地给出了 FGM 结构在磁场中的电磁力模型.研究结果可为 FGM 壳体多场耦合动力学研究提供理论支持,亦可为复合结构在工程技术领域的应用提供技术储备.

1 基本模型

研究图 1 所示处于外加磁场 $\mathbf{B}(B_x, B_\theta, B_z)$ 环境中的金属-陶瓷功能梯度圆柱薄壳体结构, 设定壳体外表面为具有铁磁性质的金属材料侧(以下角标 m 表示)、内表面为陶瓷材料侧(以下角标 c 表示), 内部材料组成呈幂律分布. 在壳体几何中面上建立正交曲线坐标系 (x, θ, z) , 壳体的厚度为 h , 中面半径为 R , 长度为 l .

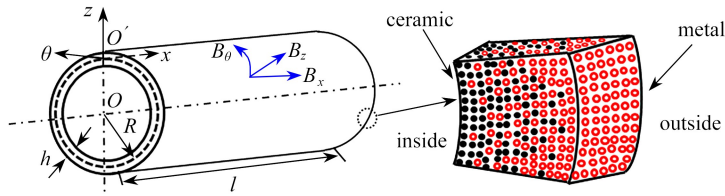


图 1 磁场中 FGM 圆柱壳模型

Fig. 1 The model for the FGM cylindrical shell in a magnetic field

1.1 材料属性

对于所研究的 FGM 壳体, 设定 V_m 为金属沿厚度方向的体积含量, V_c 为陶瓷沿厚度方向的体积含量, 则有 $V_m + V_c = 1$; N 为金属材料的体积分数指数 ($0 \leq N < \infty$); 壳体材料的物性参数主要包括弹性模量 E 、热膨胀系数 α 、密度 ρ 和 Poisson 比 ν . 设金属含量 V_m 沿厚度方向按幂律函数形式变化, 即^[31]

$$V_m = 1 - V_c = \left(\frac{h + 2z}{2h} \right)^N. \quad (1)$$

根据材料混合律, 物性参数的统一表示式为

$$P = P_c V_c + P_m V_m = (P_m - P_c) \left(\frac{h + 2z}{2h} \right)^N + P_c. \quad (2)$$

1.2 物理中面

对于沿厚度方向材料组分梯度变化的功能梯度壳体, 因材料组成结构的非对称特征, 使得弯曲应力和应变为零的圆壳面会偏离壳体的几何中曲面, 该圆柱面称为物理中曲面. 基于物理中面分析时可避免 FGM 结构中的拉伸-弯曲耦合效应. 根据等效弹性模量 E 的概念, 物理中曲面位置坐标定义为^[32]

$$z_0 = \frac{\int_{-h/2}^{h/2} z \cdot E(z) dz}{\int_{-h/2}^{h/2} E(z) dz}, \quad (3)$$

式中, z_0 为沿 z 方向物理中曲面与几何中曲面的距离.

根据 Kirchhoff 经典板壳理论, 基于物理中面的壳体内任一点位移可表示为

$$\begin{cases} u_x = u(x, \theta, t) + (z - z_0)\psi_x(x, \theta, t), \\ u_\theta = v(x, \theta, t) + (z - z_0)\psi_\theta(x, \theta, t), \\ u_z = w(x, \theta, t), \end{cases} \quad (4)$$

式中, u, v 和 w 分别为物理中曲面上点沿坐标 x, θ 和 z 方向的位移; t 为时间变量; $\psi_x = -w_{,x}, \psi_\theta = (v - w_{,\theta})/R$ 分别为物理中曲面法线沿 x 和 θ 方向的转角; $w_{,x}$ 和 $w_{,\theta}$ 的下角标“,” 分别表示对变量 x 和 θ 的一阶偏导数(下同).

2 应变能与动能

2.1 几何方程

根据 Love 板壳弹性理论, 圆柱薄壳体在几何非线性下基于物理中曲面的应变-位移关系可表示为

$$\boldsymbol{\varepsilon} = \boldsymbol{\varepsilon}^0 + (z - z_0)\boldsymbol{\varepsilon}^1, \quad (5)$$

式中, $\boldsymbol{\varepsilon} = \{\varepsilon_x, \varepsilon_\theta, \gamma_{x\theta}\}^T$ 为体内任一点应变, $\boldsymbol{\varepsilon}^0 = \{\varepsilon_x^0, \varepsilon_\theta^0, \gamma_{x\theta}^0\}^T$ 为物理中面应变, $\boldsymbol{\varepsilon}^1 = \{\kappa_x, \kappa_\theta, \kappa_{x\theta}\}^T$ 为物

理中面曲率,且有

$$\varepsilon_x^0 = u_{,x} + \frac{1}{2}(w_{,x})^2, \varepsilon_\theta^0 = \frac{v_{,\theta}}{R} + \frac{w}{R} + \frac{1}{2}\left(\frac{w_{,\theta}}{R}\right)^2, \gamma_{x\theta}^0 = \frac{u_{,\theta}}{R} + v_{,x} + \frac{w_{,x}w_{,\theta}}{R}, \quad (6)$$

$$\kappa_x = -w_{,xx}, \kappa_\theta = -\frac{w_{,\theta\theta}}{R^2} + \frac{v_{,\theta}}{R^2}, \kappa_{x\theta} = -\frac{2}{R}(w_{,x\theta} - v_{,x}), \quad (7)$$

式中, $w_{,xx}$ 的下角标“,”表示对单变量 x 的二阶偏导数, $w_{,x\theta}$ 的下角标“,”表示对双变量 x 和 θ 的二阶偏导数(下同).

2.2 物理方程

对于线弹性 FGM 壳体,根据 Hooke 定律,其应力和应变之间的弹性本构关系为

$$\boldsymbol{\sigma} = \boldsymbol{Q}\boldsymbol{\varepsilon}, \quad (8)$$

式中, $\boldsymbol{\sigma} = \{\sigma_x, \sigma_\theta, \sigma_{x\theta}\}^T$ 为壳体内任一点应力, $\boldsymbol{Q} = \frac{E}{1-\nu^2} \begin{bmatrix} 1 & \nu & 0 \\ \nu & 1 & 0 \\ 0 & 0 & (1-\nu)/2 \end{bmatrix}$ 为刚度矩阵.

对式(8)沿壳体厚度方向积分,得到等效于壳体物理中面的薄膜内力和内力矩关系式:

$$\begin{cases} (N_x, N_\theta, N_{x\theta})^T = \int_{-h/2}^{h/2} \boldsymbol{\sigma} dz = \boldsymbol{A}\boldsymbol{\varepsilon}^0, \\ (M_x, M_\theta, M_{x\theta})^T = \int_{-h/2}^{h/2} (z - z_0) \boldsymbol{\sigma} dz = \boldsymbol{D}\boldsymbol{\varepsilon}^1, \end{cases} \quad (9)$$

式中, $N_x, N_\theta, N_{x\theta}$ 为薄膜内力, $M_x, M_\theta, M_{x\theta}$ 为内力矩,刚度矩阵 $\boldsymbol{A}, \boldsymbol{D}$ 为

$$(\boldsymbol{A}, \boldsymbol{D}) = \int_{-h/2}^{h/2} \boldsymbol{Q}(1, (z - z_0)^2) dz. \quad (10)$$

2.3 应变能及变分

根据弹性应变能概念,FGM 圆柱薄壳体的应变能表达式为

$$U = \frac{1}{2} \int_0^l \int_0^{2\pi} (N_x \varepsilon_x^0 + N_\theta \varepsilon_\theta^0 + N_{x\theta} \gamma_{x\theta}^0 + M_x \kappa_x + M_\theta \kappa_\theta + M_{x\theta} \kappa_{x\theta}) R d\theta dx. \quad (11)$$

对式(11)进行变分,并考虑到内力与应变关系以及各位移变分量 $\delta u, \delta v, \delta w$ 的相互独立条件,推得体内应变能的变分式为

$$\begin{aligned} \delta U = & - \int_0^l \int_0^{2\pi} \left\{ \left(N_{x,x} + \frac{N_{x\theta,\theta}}{R} \right) \delta u + \left(\frac{N_{\theta,\theta}}{R} + N_{x\theta,x} + \frac{M_{\theta,\theta}}{R^2} + \frac{2M_{x\theta,x}}{R} \right) \delta v + \right. \\ & \left[\left(N_x w_{,x} \right)_{,x} - \frac{N_\theta}{R} + \frac{1}{R^2} (N_\theta w_{,\theta})_{,\theta} + \frac{1}{R} (N_{x\theta} w_{,x})_{,\theta} + \frac{1}{R} (N_{x\theta} w_{,\theta})_{,x} + \right. \\ & \left. \left. M_{x,xx} + \frac{M_{\theta,\theta\theta}}{R^2} + \frac{2M_{x\theta,x\theta}}{R} \right] \delta w \right\} R d\theta dx, \end{aligned} \quad (12)$$

式中, δU 为应变能变分.

2.4 动能及变分

壳体运动变形时,其内部任意一点速度矢量为

$$\boldsymbol{V} = \dot{u}_x \boldsymbol{e}_1 + \dot{u}_\theta \boldsymbol{e}_2 + \dot{u}_z \boldsymbol{e}_3, \quad (13)$$

式中, $\dot{u}_x = \frac{\partial u_x}{\partial t}$, $\dot{u}_\theta = \frac{\partial u_\theta}{\partial t}$, $\dot{u}_z = \frac{\partial w}{\partial t}$; $(\boldsymbol{e}_1, \boldsymbol{e}_2, \boldsymbol{e}_3)$ 为沿坐标 (x, θ, z) 方向的单位向量.从而得到壳体的动能表达式为

$$T = \frac{1}{2} \iiint \rho(z) \cdot \boldsymbol{V} \cdot \boldsymbol{V} \cdot R d\theta dx dz = \frac{1}{2} \iiint \rho(z) \cdot (\dot{u}_x^2 + \dot{u}_\theta^2 + \dot{u}_z^2) R dx d\theta dz. \quad (14)$$

将式(4)代入式(14),对动能进行变分运算,并考虑到 $\delta u, \delta v, \delta w$ 为独立变分量,得到动能变分式 δT 为

$$\delta T = - \int_0^l \int_0^{2\pi} \left\{ \left[I_0 \frac{\partial^2 u}{\partial t^2} - I_1 \frac{\partial^2}{\partial t^2} (w_{,x}) \right] \delta u + \left[I_0 \frac{\partial^2 v}{\partial t^2} + \frac{I_1}{R} \left(2 \frac{\partial^2 v}{\partial t^2} - \frac{\partial^2 w_{,\theta}}{\partial t^2} \right) + \frac{I_2}{R^2} \frac{\partial^2 (v - w_{,\theta})}{\partial t^2} \right] \delta v + \left[I_0 \frac{\partial^2 w}{\partial t^2} + \frac{I_1}{R} \left(R \frac{\partial^2 u_{,x}}{\partial t^2} + \frac{\partial^2 v_{,\theta}}{\partial t^2} \right) + \frac{I_2}{R^2} \left(\frac{\partial^2 (v_{,\theta} - w_{,\theta\theta})}{\partial t^2} - R^2 \frac{\partial^2 w_{,xx}}{\partial t^2} \right) \right] \delta w \right\} R d\theta dx, \quad (15)$$

式中

$$I_0 = \int_{-h/2}^{h/2} \rho(z) \cdot dz, \quad I_1 = \int_{-h/2}^{h/2} \rho(z) \cdot (z - z_0) dz, \quad I_2 = \int_{-h/2}^{h/2} \rho(z) \cdot (z - z_0)^2 dz. \quad (16)$$

3 电磁力模型

3.1 Lorentz 力

当运动导体处于外加磁场作用时,电磁体内部将会因动变形而产生感应涡电流,其电流密度的矢量表征式为

$$\mathbf{J} = \sigma(z) \cdot (\mathbf{V}_p \times \mathbf{B}), \quad (17)$$

式中, $\mathbf{J}(J_x, J_\theta, J_z)$ 为电流密度矢量, $\mathbf{B}(B_x, B_\theta, B_z)$ 为磁感应强度矢量, $\mathbf{V}_p(V_{px}, V_{p\theta}, V_{pz})$ 为任一点速度矢量;

$\sigma(z) = \sigma_m V_m = \sigma_m \left(\frac{1}{2} + \frac{z}{h} \right)^N$ 为沿壳体厚度呈幂律梯度变化的电导率, σ_m 为金属材料电导率。

基于电磁理论,FGM 薄壳体在外加磁场环境中所受到的 Lorentz 力矢量式为^[23]

$$\mathbf{f}^L(f_x^L, f_\theta^L, f_z^L) = \mathbf{J} \times \mathbf{B} = \begin{vmatrix} \mathbf{e}_1 & \mathbf{e}_2 & \mathbf{e}_3 \\ J_x & J_\theta & 0 \\ B_x & B_\theta & B_z \end{vmatrix}. \quad (18)$$

将 Lorentz 力矢量式(18)沿壳体厚度方向对 z 进行积分,推得等效于壳体物理中面的涡流电磁力和电磁力矩:

$$\begin{cases} F_x^L = \int_{-h/2}^{h/2} f_x^L dz = \frac{\partial w}{\partial t} \hat{B}_{xz}^0 - \frac{\partial u}{\partial t} \hat{B}_{zz}^0 - \frac{\partial \psi_x}{\partial t} \hat{B}_{zz}^1, \\ F_\theta^L = \int_{-h/2}^{h/2} f_\theta^L dz = -\frac{\partial v}{\partial t} \hat{B}_{zz}^0 - \frac{\partial \psi_\theta}{\partial t} \hat{B}_{zz}^1 + \frac{\partial w}{\partial t} \hat{B}_{\theta z}^0, \\ F_z^L = \int_{-h/2}^{h/2} f_z^L dz = \frac{\partial v}{\partial t} \hat{B}_{\theta z}^0 + \frac{\partial \psi_\theta}{\partial t} \hat{B}_{\theta z}^1 - \frac{\partial w}{\partial t} \hat{B}_{\theta\theta}^0 - \frac{\partial w}{\partial t} \hat{B}_{xx}^0 + \frac{\partial u}{\partial t} \hat{B}_{xz}^0 + \frac{\partial \psi_x}{\partial t} \hat{B}_{xz}^1, \\ m_x^L = \int_{-h/2}^{h/2} f_x^L \cdot (z - z_0) dz = \frac{\partial w}{\partial t} \hat{B}_{xz}^1 - \frac{\partial u}{\partial t} \hat{B}_{zz}^1 - \frac{\partial \psi_x}{\partial t} \hat{B}_{zz}^{\text{II}}, \\ m_\theta^L = \int_{-h/2}^{h/2} f_\theta^L \cdot (z - z_0) dz = -\frac{\partial v}{\partial t} \hat{B}_{zz}^1 - \frac{\partial \psi_\theta}{\partial t} \hat{B}_{zz}^{\text{II}} + \frac{\partial w}{\partial t} \hat{B}_{\theta z}^1, \end{cases} \quad (19)$$

式中

$$\begin{aligned} \hat{B}_{xz}^0 &= \int_{-h/2}^{h/2} \sigma B_x B_z dz, \quad \hat{B}_{\theta z}^0 = \int_{-h/2}^{h/2} \sigma B_\theta B_z dz, \quad \hat{B}_{xx}^0 = \int_{-h/2}^{h/2} \sigma B_x^2 dz, \quad \hat{B}_{\theta\theta}^0 = \int_{-h/2}^{h/2} \sigma B_\theta^2 dz, \\ \hat{B}_{zz}^0 &= \int_{-h/2}^{h/2} \sigma B_z^2 dz, \quad \hat{B}_{zz}^1 = \int_{-h/2}^{h/2} \sigma B_z^2 \cdot (z - z_0) dz, \quad \hat{B}_{xz}^1 = \int_{-h/2}^{h/2} \sigma B_x B_z \cdot (z - z_0) dz, \\ \hat{B}_{\theta z}^1 &= \int_{-h/2}^{h/2} \sigma B_\theta B_z \cdot (z - z_0) dz, \quad \hat{B}_{zz}^{\text{II}} = \int_{-h/2}^{h/2} \sigma B_z^2 \cdot (z - z_0)^2 dz. \end{aligned}$$

3.2 磁化力

3.2.1 电磁本构关系和磁边界条件

对于各向同性铁磁材料介质,其电磁本构式为

$$\begin{cases} \mathbf{B} = \mu \mathbf{H} = \mu_0 (\mathbf{H} + \mathbf{M}), \\ \mathbf{M} = \chi \mathbf{H}, \end{cases} \quad (21)$$

式中, $\mu = \mu_0 \mu_r$ 为介质磁导率, $\mu_r = 1 + \chi$ 为相对磁导率, μ_0 为真空磁导率, $\chi(z) = \chi_m V_m = \chi_m \left(\frac{1}{2} + \frac{z}{h} \right)^N$ 为沿壳体厚度呈幂律梯度变化的磁化率, χ_m 为金属材料磁化率; \mathbf{M} 为磁化强度矢量, \mathbf{H} 为磁场强度矢量。

根据电磁理论, 壳体介质表面磁场的连续性边界条件为

$$\bar{B}_m^z = B_m^z, \quad \bar{H}_m^r = H_m^r, \quad (22)$$

式中, \bar{B}_m^z, B_m^z 分别为体内和体外边界沿法向的磁感应强度, \bar{H}_m^r, H_m^r 分别为体内和体外边界沿切向的磁场强度, 下角标“m”代表壳体的外表面(金属侧)。

3.2.2 磁力模型

基于磁介质的微观磁偶极子理论, 对于各向同性可磁化铁磁材料薄壁结构, 其介质所受的磁体力和表面磁力的表征式为^[23]:

磁体力

$$\mathbf{f}^C(f_x^C, f_\theta^C, f_z^C) = \frac{\mu_0 \mu_r \chi}{2} \nabla(\mathbf{H})^2; \quad (23)$$

磁面力

$$\mathbf{f}_1^C = -\frac{\mu_0 \chi (\mu_r + 1)}{2} (\bar{H}^r)^2 \mathbf{n}, \quad (24)$$

式中, \mathbf{n} 为外法向单位向量, ∇ 为柱坐标系下的 Hamilton 微分算子。

当研究薄壁壳体时, 可将磁体力(23)和磁面力(24)向物理中面等效简化, 得到壳体所受的磁化力和磁化力矩表达式:

$$\begin{cases} F_x^C = \int_{-h/2}^{h/2} f_x^C dz = \frac{\mu_0}{2} \int_{-h/2}^{h/2} \mu_r(z) \cdot \chi(z) \cdot [(\mathbf{H})^2]_{,x} dz, \\ F_\theta^C = \int_{-h/2}^{h/2} f_\theta^C dz = \frac{\mu_0}{2R} \int_{-h/2}^{h/2} \mu_r(z) \cdot \chi(z) \cdot [(\mathbf{H})^2]_{,\theta} dz, \\ F_z^C = \int_{-h/2}^{h/2} f_z^C dz + \bar{f}_1^C \Big|_{z=h/2} - \bar{f}_1^C \Big|_{z=-h/2} = \\ \frac{\mu_0}{2} \int_{-h/2}^{h/2} \mu_r(z) \cdot \chi(z) \cdot [(\mathbf{H})^2]_{,z} dz - \frac{\mu_0 \chi (\mu_r + 1)}{2} (\bar{H}^r)^2 \Big|_{z=-h/2}^{z=h/2}, \end{cases} \quad (25)$$

$$\begin{cases} m_x^C = \int_{-h/2}^{h/2} f_x^C \cdot (z - z_0) dz = \frac{\mu_0}{2} \int_{-h/2}^{h/2} \mu_r(z) \cdot \chi(z) \cdot [(\mathbf{H})^2]_{,x} \cdot (z - z_0) dz, \\ m_\theta^C = \int_{-h/2}^{h/2} f_\theta^C \cdot (z - z_0) dz = \frac{\mu_0}{2R} \int_{-h/2}^{h/2} \mu_r(z) \cdot \chi(z) \cdot [(\mathbf{H})^2]_{,\theta} \cdot (z - z_0) dz. \end{cases} \quad (26)$$

3.3 电磁力虚功

设壳体所受总的等效电磁体力(包括 Lorentz 力和磁化力)为

$$\mathbf{f} = f_x \mathbf{e}_1 + f_\theta \mathbf{e}_2 + f_z \mathbf{e}_3, \quad (27)$$

则对于系统约束所容许的虚位移, 电磁力所做虚功为

$$\begin{aligned} \delta W = \int_0^l \int_0^{2\pi} \int_{-h/2}^{h/2} (f_x \delta u_x + f_\theta \delta u_\theta + f_z \delta u_z) R dz d\theta dx = \\ \int_0^l \int_0^{2\pi} \left[F_x \delta u + \left(F_\theta + \frac{m_\theta}{R} \right) \delta v + \left(F_z + m_{x,x} + \frac{m_{\theta,\theta}}{R} \right) \delta w \right] R d\theta dx, \end{aligned} \quad (28)$$

式中, δW 为电磁力虚功, 沿 z 方向积分后等效于物理中面的电磁力 F_x, F_θ, F_z 和电磁力矩 m_x, m_θ 分别为

$$\begin{cases} F_x = F_x^L + F_x^C, & F_\theta = F_\theta^L + F_\theta^C, & F_z = F_z^L + F_z^C, \\ m_x = m_x^L + m_x^C, & m_\theta = m_\theta^L + m_\theta^C, \end{cases} \quad (29)$$

这里, 上角标“L”代表 Lorentz 力, “C”代表磁化力, 其表达式见式(19)、(20)和式(25)、(26)。

4 磁弹耦合非线性振动方程

对于弹性变形薄壳体,可应用 Hamilton 广义变分原理建立电磁场作用下 FGM 结构的非线性振动方程。

Hamilton 变分原理的一般表达形式为

$$\int_{t_1}^{t_2} (\delta T - \delta U + \delta W) dt = 0, \quad (30)$$

式中, t_1 和 t_2 为两个积分限固定时刻。

最终,将前面所得变分式(12)、(15)和虚功式(28)代入 Hamilton 变分原理(30)中,并考虑到 $\delta u, \delta v, \delta w$ 为独立的位移变分量,推得电磁场环境中功能梯度薄壳体的磁弹耦合非线性振动方程组:

$$N_{x,x} + \frac{N_{x\theta,\theta}}{R} + F_x = I_0 \frac{\partial^2 u}{\partial t^2} - I_1 \frac{\partial^2 w_{,x}}{\partial t^2}, \quad (31)$$

$$\frac{N_{\theta,\theta}}{R} + N_{x\theta,x} + \frac{1}{R^2} M_{\theta,\theta} + \frac{2M_{x\theta,x}}{R} + F_\theta + \frac{m_\theta}{R} = I_0 \frac{\partial^2 v}{\partial t^2} + \frac{I_1}{R} \left(2 \frac{\partial^2 v}{\partial t^2} - \frac{\partial^2 w_{,\theta}}{\partial t^2} \right) + \frac{I_2}{R^2} \frac{\partial^2 (v - w_{,\theta})}{\partial t^2}, \quad (32)$$

$$\begin{aligned} & (N_x w_{,x})_{,x} - \frac{N_\theta}{R} + \frac{1}{R^2} (N_\theta w_{,\theta})_{,\theta} + \frac{1}{R} (N_{x\theta} w_{,x})_{,\theta} + \frac{1}{R} (N_{x\theta} w_{,\theta})_{,x} + \\ & M_{x,xx} + \frac{M_{\theta,\theta\theta}}{R^2} + \frac{2M_{x\theta,x\theta}}{R} + F_z + m_{x,x} + \frac{m_{\theta,\theta}}{R} = \\ & I_0 \frac{\partial^2 w}{\partial t^2} + \frac{I_1}{R} \left(R \frac{\partial^2 u_{,x}}{\partial t^2} + \frac{\partial^2 v_{,\theta}}{\partial t^2} \right) + \frac{I_2}{R^2} \left[\frac{\partial^2 (v_{,\theta} - w_{,\theta\theta})}{\partial t^2} - R^2 \frac{\partial^2 w_{,xx}}{\partial t^2} \right]. \end{aligned} \quad (33)$$

综上,非线性振动方程组(31)–(33)及其对应的关系式,即构成了表征变形场与电磁场相互作用下功能梯度薄壳体的磁弹耦合动力学理论模型。

5 固有振动特性

本节以横向恒定磁场 $B = B_0$ 中两端简支约束下功能梯度圆柱壳的固有振动问题为例进行研究,且仅考虑几何线性情况,给出振动特征方程和不同参量对系统固有振动频率的影响规律。

5.1 固有振动特征方程

基于几何方程(5)、物理方程(9)并考虑电磁力表达式(29),可将功能梯度圆柱壳方程(31)–(33)简化为如下以扰动位移表示的横向磁场环境中的振动微分方程组:

$$\begin{cases} L_{11}u + L_{12}v + L_{13}w = 0, \\ L_{21}u + L_{22}v + L_{23}w = 0, \\ L_{31}u + L_{32}v + L_{33}w = 0, \end{cases} \quad (34)$$

式中

$$\begin{aligned} L_{11} &= A_{11} \frac{\partial^2}{\partial x^2} + A_{33} \frac{\partial^2}{R^2 \partial \theta^2} - \hat{B}_{zz}^0 \frac{\partial}{\partial t} - I_0 \frac{\partial^2}{\partial t^2}, \quad L_{12} = A_{12} \frac{\partial^2}{R \partial \theta \partial x} + A_{33} \frac{\partial^2}{R \partial \theta \partial x}, \\ L_{13} &= A_{12} \frac{\partial}{R \partial x} + \hat{B}_{zz}^1 \frac{\partial^2}{\partial x \partial t} + I_1 \frac{\partial^3}{\partial t^2 \partial x}, \quad L_{21} = A_{21} \frac{\partial^2}{R \partial \theta \partial x} + A_{33} \frac{\partial^2}{R \partial \theta \partial x}, \\ L_{22} &= A_{22} \frac{\partial^2}{R^2 \partial \theta^2} + A_{33} \frac{\partial^2}{\partial x^2} - \hat{B}_{zz}^0 \frac{\partial}{\partial t} - I_0 \frac{\partial^2}{\partial t^2}, \quad L_{23} = A_{22} \frac{\partial}{R^2 \partial \theta} + \hat{B}_{zz}^1 \frac{\partial^2}{R \partial \theta \partial t} + I_1 \frac{\partial^3}{R \partial t^2 \partial \theta}, \\ L_{31} &= -A_{21} \frac{\partial}{R \partial x} - \hat{B}_{zz}^1 \frac{\partial^2}{\partial t \partial x} - I_1 \frac{\partial^3}{\partial t^2 \partial x}, \quad L_{32} = -A_{22} \frac{\partial}{R^2 \partial \theta} - \hat{B}_{zz}^1 \frac{\partial^2}{R \partial \theta \partial t} - I_1 \frac{\partial^3}{R \partial t^2 \partial \theta}, \\ L_{33} &= -\frac{A_{22}}{R^2} - D_{11} \frac{\partial^4}{\partial x^4} - D_{12} \frac{\partial^4}{R^2 \partial x^2 \partial \theta^2} - D_{21} \frac{\partial^4}{R^2 \partial x^2 \partial \theta^2} - D_{22} \frac{\partial^4}{R^4 \partial \theta^4} - 4D_{33} \frac{\partial^4}{R^2 \partial x^2 \partial \theta^2} + \end{aligned}$$

$$\hat{B}_{zz}^{\parallel} \frac{\partial^3}{\partial x^2 \partial t} + \hat{B}_{zz}^{\parallel} \frac{\partial^3}{R^2 \partial \theta^2 \partial t} - I_0 \frac{\partial^2}{\partial t^2} + I_2 \frac{1}{R^2} \left(R^2 \frac{\partial^4}{\partial t^2 \partial x^2} + \frac{\partial^4}{\partial t^2 \partial \theta^2} \right),$$

这里,磁场作用量积分式 $\hat{B}_{zz}^0 = \int_{-h/2}^{h/2} \sigma B_{0z}^2 dz$, $\hat{B}_{zz}^1 = \int_{-h/2}^{h/2} \sigma B_{0z}^2 \cdot (z - z_0) dz$, $\hat{B}_{zz}^{\parallel} = \int_{-h/2}^{h/2} \sigma B_{0z}^2 \cdot (z - z_0)^2 dz$; $I_i (i = 0, 1, 2)$ 为式(16)表示的密度积分定义式; $A_{ij} (i, j = 1, 2)$ 、 A_{33} 、 $D_{ij} (i, j = 1, 2)$ 和 D_{33} 为式(10)表示的刚度矩阵对应元素。

对于两端简支边界约束的 FGM 圆柱壳,其边界条件为

$$\begin{cases} x = 0: v = 0, w = 0, N_x = 0, M_x = 0, \\ x = l: v = 0, w = 0, N_x = 0, M_x = 0. \end{cases} \quad (35)$$

根据模态展开法,将满足边界条件(35)的关于壳体振动方程(34)的位移解取为如下变量分离形式:

$$\begin{cases} u(x, \theta, t) = \sum_{m=1}^{\infty} \sum_{n=1}^{\infty} r(t) \frac{m\pi}{l} \cos \frac{m\pi x}{l}, \\ v(x, \theta, t) = \sum_{m=1}^{\infty} \sum_{n=1}^{\infty} p(t) \sin \frac{m\pi x}{l}, \\ w(x, \theta, t) = \sum_{m=1}^{\infty} \sum_{n=1}^{\infty} q(t) \sin \frac{m\pi x}{l}, \end{cases} \quad (36)$$

其中, $r(t)$ 为轴向位移振幅, $p(t)$ 为周向位移振幅, $q(t)$ 为横向位移振幅, m 和 n 分别为轴向和周向波数。

将式(36)代入式(34)中,进行 Galerkin 内积离散得到关于 u, v, w 方向的振动微分方程:

$$\begin{cases} \ddot{r}(t) + a_1 \dot{r}(t) + a_2 r(t) = a_3 p(t) + a_4 q(t) + a_5 \dot{q}(t) + a_6 \ddot{q}(t), \\ \ddot{p}(t) + b_1 \dot{p}(t) + b_2 p(t) = b_3 r(t) + b_4 q(t) + b_5 \dot{q}(t) + b_6 \ddot{q}(t), \\ \ddot{q}(t) + c_1 \dot{q}(t) + c_2 q(t) = c_3 r(t) + c_4 \dot{r}(t) + c_5 \ddot{r}(t) + c_6 p(t) + c_7 \dot{p}(t) + c_8 \ddot{p}(t), \end{cases} \quad (37)$$

式中

$$\begin{aligned} a_1 &= \frac{\hat{B}_{zz}^0}{I_0}, a_2 = \frac{A_{11}}{I_0} \left(\frac{m\pi}{l} \right)^2 + \frac{A_{33} n^2}{I_0 R^2}, a_3 = \frac{(A_{12} + A_{33}) n}{I_0 R}, a_4 = \frac{A_{12}}{I_0 R}, a_5 = \frac{\hat{B}_{zz}^1}{I_0}, a_6 = -\frac{I_1}{I_0}, \\ b_1 &= \frac{\hat{B}_{zz}^0}{I_0}, b_2 = \frac{A_{22} n^2}{I_0 R^2} - \frac{A_{33}}{I_0} \left(\frac{m\pi}{l} \right)^2, b_3 = (A_{21} + A_{33}) \frac{n}{I_0 R} \left(\frac{m\pi}{l} \right)^2, \\ b_4 &= -\frac{A_{22} n}{I_0 R^2}, b_5 = -\frac{\hat{B}_{zz}^1 n}{I_0 R}, b_6 = -\frac{I_1 n}{I_0 R}, I = I_0 + I_2 \left(\frac{m\pi}{l} \right)^2 + \frac{I_2 n^2}{R^2}, \\ c_1 &= \frac{\hat{B}_{zz}^{\parallel}}{I} \left(\left(\frac{m\pi}{l} \right)^2 + \frac{n^2}{R^2} \right), c_2 = \frac{A_{22}}{IR^2} + \frac{D_{11}}{I} \left(\frac{m\pi}{l} \right)^4 + \frac{2D_{12} n^2}{IR^2} \left(\frac{m\pi}{l} \right)^2 + \frac{D_{22} n^4}{R^4} + \frac{4D_{33} n^2}{IR^2} \left(\frac{m\pi}{l} \right)^2, \\ c_3 &= \frac{A_{21}}{IR} \left(\frac{m\pi}{l} \right)^2, c_4 = \frac{\hat{B}_{zz}^1}{I} \left(\frac{m\pi}{l} \right)^2, c_5 = \frac{I_1}{I} \left(\frac{m\pi}{l} \right)^2, c_6 = \frac{A_{22} n}{IR^2}, c_7 = -\frac{\hat{B}_{zz}^1 n}{IR}, c_8 = -\frac{I_1 n}{IR}. \end{aligned}$$

令 $r(t) = U_{mn} e^{i(n\theta + \omega_{mn} t)}$, $p(t) = V_{mn} e^{i(\pi/2 + n\theta + \omega_{mn} t)}$, $q(t) = W_{mn} e^{i(n\theta + \omega_{mn} t)}$, 其中 U_{mn} , V_{mn} 和 W_{mn} 分别代表轴向、周向和法向的待定幅值系数,将其代入式(37),再根据系数 U_{mn} , V_{mn} 和 W_{mn} 满足非平凡解的条件,得到横向磁场中功能梯度壳体的固有振动特征方程:

$$\begin{vmatrix} \omega_{mn}^2 - ia_1 \omega_{mn} - a_2 & & -a_3 & a_6 \omega_{mn}^2 + ia_5 \omega_{mn} - a_4 \\ & -b_3 & \omega_{mn}^2 - ib_1 \omega_{mn} - b_2 & b_6 \omega_{mn}^2 + ib_5 \omega_{mn} - b_4 \\ -c_5 \omega_{mn}^2 + ic_4 \omega_{mn} + c_3 & c_8 \omega_{mn}^2 - ic_7 \omega_{mn} - c_6 & \omega_{mn}^2 - ic_1 \omega_{mn} - c_2 & \end{vmatrix} = 0. \quad (38)$$

5.2 算例结果及分析

选取外侧为金属 Bi、内侧为陶瓷材料 Si_3N_4 组成的 FGM 圆柱壳进行计算分析,其组成成分的物理参数和结构参数分别为:Bi, $\rho = 9750 \text{ kg/m}^3$, $\sigma_m = 8.67 \times 10^5 (\Omega \cdot \text{m})^{-1}$, $\nu = 0.33$, $E = 32 \text{ GPa}$; Si_3N_4 , $\rho = 2370$

$\text{kg/m}^3, \nu = 0.24, E = 320 \text{ GPa}; R = 0.2 \text{ m}, h = 0.002 \text{ m}, l = 1.4 \text{ m}$. 下面通过对特征方程 (38) 的求解, 给出横向磁场中功能梯度圆柱壳的固有振动频率值, 且在对应每一组 (m, n) 的频率 ω_{mn} 中取其最小值结果, 分析不同参量对该频率值的影响规律.

图 2 给出了功能梯度圆柱壳固有频率随周向波数变化的特征曲线. 图 2(a) 取 $N = 0.1, m = 1$; 图 2(b) 取 $B_{0z} = 5 \text{ T}, N = 0.1$; 图 2(c) 取 $B_{0z} = 5 \text{ T}, m = 1$. 由图 2 可见, 随着不同参量的改变, 固有频率随着周向波数的增加均呈现先减小后增大的趋势. 这是由于在壳体的非轴对称运动中, 振型函数随周向波数 n 的改变发生变化, 进而影响系统的固有频率, 并且参数不同时频率最小值对应的周向波数也会发生改变. 图 2(a) 表明, 随着磁感应强度的增加, 圆柱壳受到的 Lorentz 力增大, 磁场发挥的阻尼作用增大, 使固有频率减小, 且随着周向波数的增加, 磁场对频率的影响逐渐减小, 在 $n = 1$ 和 $n = 2$ 时, 固有频率变化较为明显; 图 2(b) 表明, 随着轴向波数的增加, 固有频率增大, 但随周向波数的增加, 轴向波数对固有频率的影响逐渐减小, 说明轴向波数对圆柱壳固有频率的影响主要表现在周向波数较小的情况下; 图 2(c) 表明, 随着体积分指数增加, 金属在功能梯度圆柱壳中的组分占比减小, 壳体受到磁场的电磁阻尼效应衰减, 固有频率增大, 并且在 $n = 1$ 和 $n = 2$ 时, 体积分指数对频率的影响随周向波数增大而减小, 在 $n \geq 3$ 时, 其影响随周向波数增大而增强.

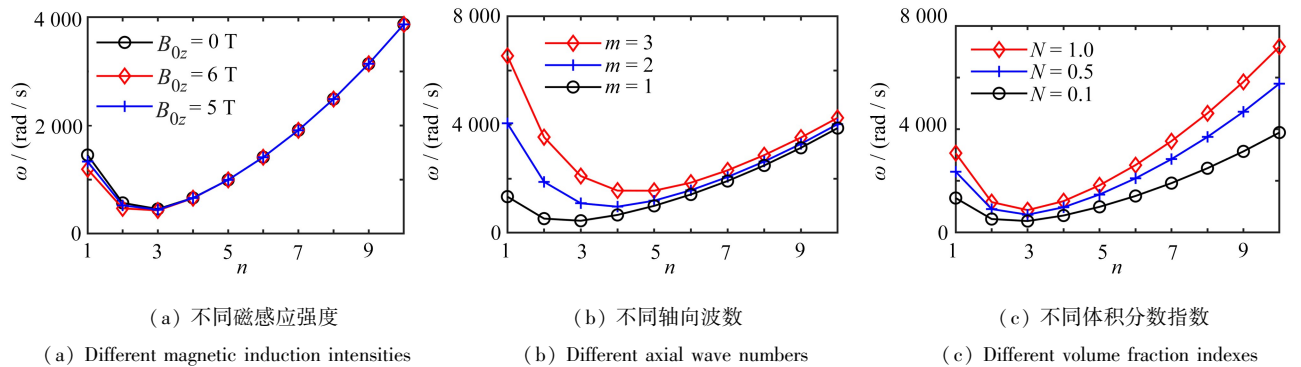


图 2 固有频率-周向波数特征曲线

Fig. 2 Characteristic curves of natural frequency-circumferential wave numbers

图 3 给出了功能梯度圆柱壳固有频率随磁感应强度变化的特征曲线. 图 3(a) 取 $m = 1, n = 3$; 图 3(b) 取 $N = 0.1, n = 3$; 图 3(c) 取 $N = 0.1, m = 1$. 由图 3 可见, 随着磁感应强度的增大, 固有频率随之减小. 这是由于磁场产生的 Lorentz 电磁力以电磁阻尼项形式作用于系统, 且磁化力大小呈磁感应强度平方幂次形式, 从而磁感应强度越大对固有频率的抑制作用越明显. 图 3(a) 表明, 随着体积分指数的增大, 固有频率增大, 且随着磁感应强度的增大, 功能梯度圆柱壳的体积分数增大, 金属的体积占比减小, 系统受到的电磁阻尼作用减小, 磁场对固有频率的影响减小; 图 3(b)、(c) 表明, 当仅增大轴向波数或仅增大周向波数 ($n \geq 3$) 时, 功能梯度圆柱壳的振动模式发生变化, 系统的固有频率明显增大, 这与图 2 中对应曲线的变化规律一致.

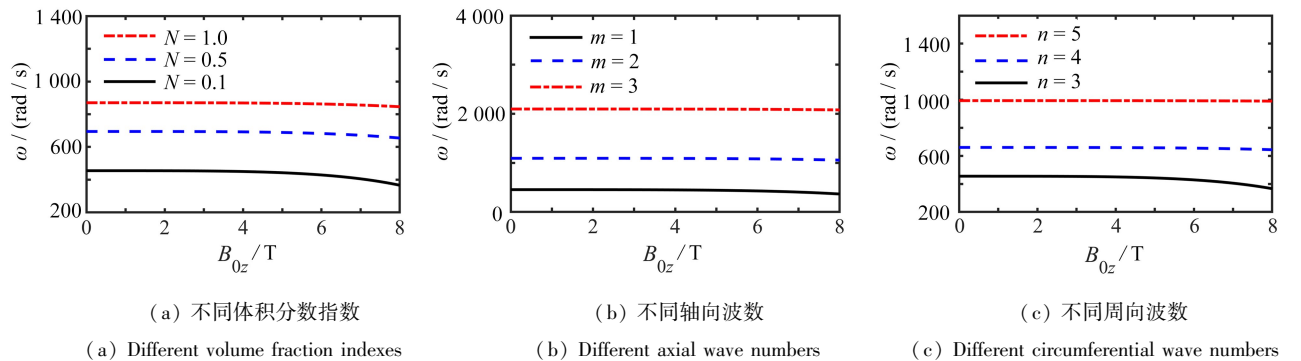


图 3 固有频率-磁感应强度特征曲线

Fig. 3 Characteristic curves of natural frequency-magnetic induction intensities

图4给出了功能梯度圆柱壳固有频率随体积分数指数变化的特征曲线。图4(a)取 $m=1, n=2$; 图4(b)取 $B_{0z}=5\text{ T}, n=2$; 图4(c)取 $B_{0z}=5\text{ T}, m=1$ 。由图4可见,固有频率随着体积分数的增大而增大,且增幅减小,这是由于纯金属圆柱壳的固有频率要低于纯陶瓷圆柱壳^[33],本文FGM圆柱壳中的金属和陶瓷在结构中的含量与体积分数呈幂指数关系,在体积分数指数较小时,功能梯度圆柱壳中金属占比较大,固有频率接近纯金属圆柱壳,增大体积分数指数,金属在功能梯度圆柱壳中的体积占比减小,陶瓷的体积占比增大,固有频率接近纯陶瓷圆柱壳。图4(a)表明,在体积分数指数较小时,金属的体积占比较大,所以磁场对功能梯度圆柱壳固有频率的阻尼作用明显,随着体积分数的增大,金属体积占比减小,磁场对固有频率影响减小;图4(b)、(c)表明,对应不变的 N 值,若轴向波数增大或周向波数减小($n \in [1, 3]$),功能梯度圆柱壳的振动模式发生变化,固有频率均呈明显的增大。

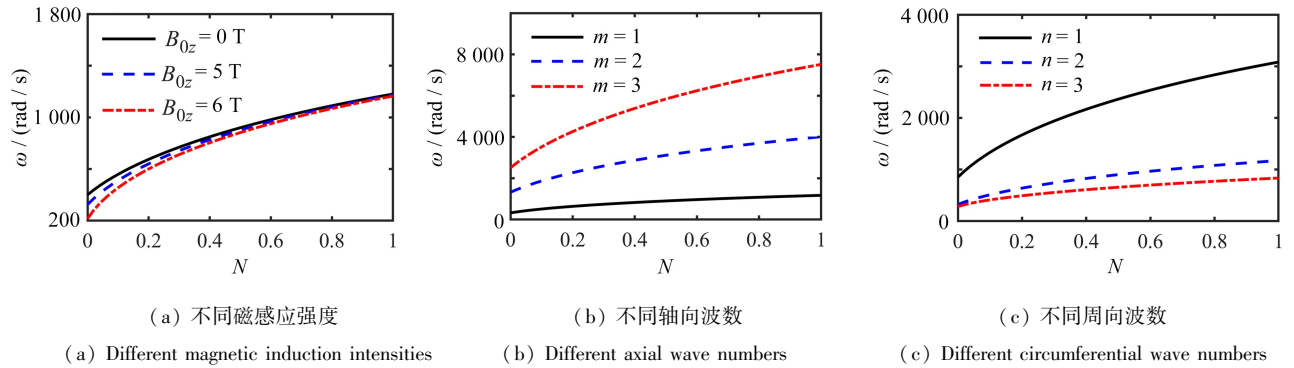


图4 固有频率-体积分数指数特征曲线

Fig. 4 Characteristic curves of natural frequency-volume fraction indexes

为研究壳体自由振动过程中磁感应强度对振幅衰减程度的影响和振动能量与固有频率之间的关系,拾取图3和图4的参考点,采用四阶Runge-Kutta方法对式(37)进行数值求解,绘制不同磁感应强度所对应的时程响应图,再利用Fourier变换绘制不同参数所对应的功率谱图。设定初始幅值 $q_0 = 8 \times 10^{-6}\text{ m}$,图5中参数为 $n=1, m=1, N=0.1$ 。由图5可知,当 $B_{0z}=0\text{ T}$ 时,系统不受电磁阻尼效应影响,表现为等幅周期性振动,随着横向磁场的增加,电磁阻尼效应逐渐明显,振幅 q 随着时间衰减直至为零。图6(a)取 $n=1, m=1, N=0.1$;图6(b)取 $n=2, m=1, B_{0z}=5\text{ T}$,图中标注 (x, y) 分别代表数值解和解析解。由图6可知,功率谱图图6(a)、(b)中数值解与图3和图4中对应参考点的解析解的固有频率值基本一致,充分说明了本文解析法所求固有频率的准确性。

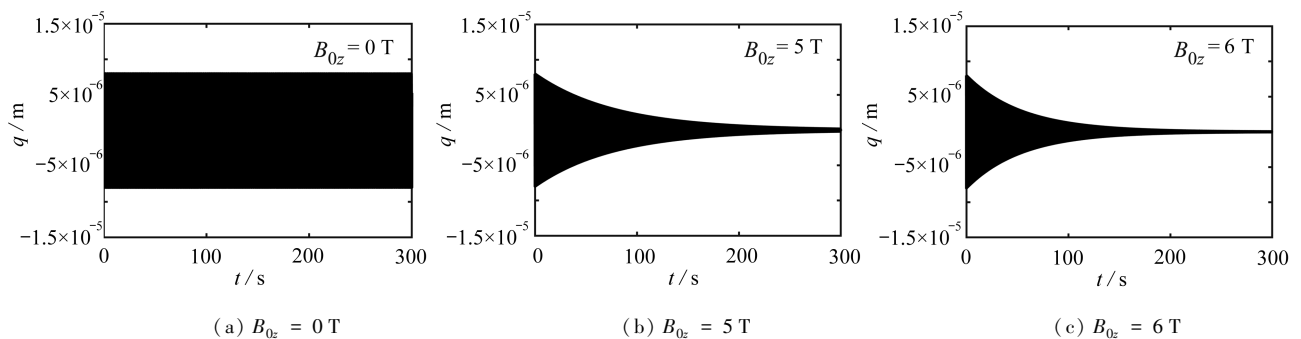


图5 不同磁感应强度FGM圆柱壳时程响应

Fig. 5 Time history response diagrams of the FGM cylindrical shell with different magnetic induction intensities

为验证本文解析结果的合理性,基于文献[34]中算例分析结果,在两端简支边界条件下,忽略外界磁场影响,选取内侧材料为镍、外侧材料为不锈钢的FGM圆柱壳,其主要参数为 $N=1, m=1, R=1\text{ m}, h/R=0.05, L/R=20$,材料其余的物性参数均取自该文献,对比结果如表1所示,本文所得FGM圆柱壳的固有频率与文献[34-35]分别采用Rayleigh-Ritz法和摄动法所获得固有频率的对比误差均在2%以内,验证结果表明了本

文理论研究的合理性.

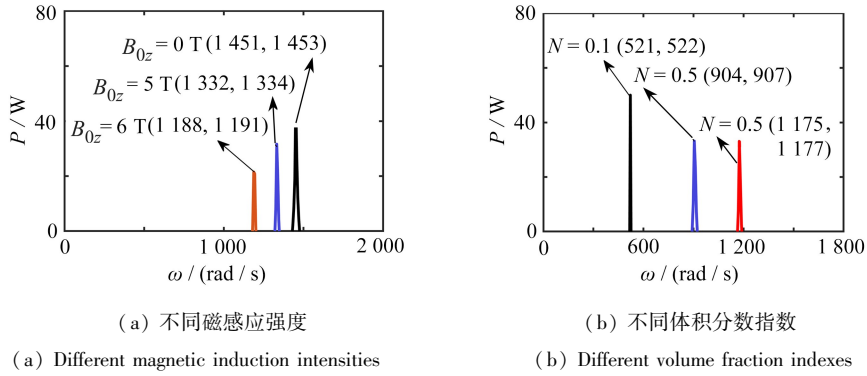


图 6 FGM 圆柱壳功率谱

Fig. 6 Power spectrum diagrams of the FGM cylindrical shell

表 1 不锈钢/镍 FGM 圆柱壳固有频率随体积分数指数变化

Table 1 Natural frequencies of stainless steel/nickel FGM shells with different volume fraction indexes

(m, n)	sources	ω / Hz				
		$N = 0$	$N = 0.5$	$N = 1$	$N = 2$	$N = 5$
(1, 7)	ref. [35]	580.70	570.25	565.46	560.93	556.45
	ref. [34]	585.79	575.27	570.48	565.92	561.40
	present	590.17	579.46	574.46	569.64	564.99
(1, 8)	ref. [35]	763.98	750.12	743.82	737.86	731.97
	ref. [34]	759.91	746.28	740.07	734.18	728.31
	present	771.37	757.37	750.82	744.54	738.46

6 结 论

本文建立了电磁场环境中非均质功能梯度壳体结构的磁弹耦合非线性动力学理论模型,并举例分析了壳体固有振动频率变化规律.研究表明:

- 1) 电磁力依赖于介质电导率和磁导率的非均匀变化而沿厚度方向呈梯度变化特征;感应涡电流引起的 Lorentz 电磁力以电磁阻尼项形式作用于系统;壳体所受磁化力呈现磁场强度的平方幂次表达形式.
- 2) 基于非均质壳体结构的物理中面分析方法,能够有效消除 FGM 复合结构中的拉伸-弯曲耦合效应,推导更为简便;动力学方程呈现运动、变形、电磁间的多场耦合机制和非线性特征.
- 3) 计算结果可见,在固有频率随周向波数变化曲线中,出现对应基频的最小值情形;磁场起到电磁阻尼作用,且随磁感应强度增大固有频率呈下降趋势;随材料体积分数指数的增加,固有频率值逐渐减小.

参考文献 (References):

[1] 沈惠申. 功能梯度复合材料板壳结构的弯曲、屈曲和振动[J]. 力学进展, 2004, **34**(1): 53-60. (SHEN Huishen. Bending, buckling and vibration of functionally graded plates and shells[J]. *Advances in Mechanics*, 2004, **34**(1): 53-60. (in Chinese))

[2] YANG B, CHEN W Q, DING H J. Approximate elasticity solutions for functionally graded circular plates subject to a concentrated force at the center[J]. *Mathematics and Mechanics of Solids*, 2014, **19**(3): 277-288.

[3] LIU N W, SUN Y L, CHEN W Q, et al. 3D elasticity solutions for stress field analysis of FGM circular plates subject to concentrated edge forces and couples[J]. *Acta Mechanica*, 2019, **230**(8): 2655-2668.

[4] YOUSEFITABAR M, MATAPOURI M K. Thermally induced buckling of thin annular FGM plates[J]. *Journal of the Brazilian Society of Mechanical Sciences and Engineering*, 2017, **39**(1): 969-980.

[5] TRABELSI S, FRIKHA A, ZGHAL S, et al. Thermal post-buckling analysis of functionally graded material

- structures using a modified FSDT[J]. *International Journal of Mechanical Sciences*, 2018, **144**(8): 74-89.
- [6] CHAN D Q, LONG V D, DUC N D. Nonlinear buckling and postbuckling of FGM shear-deformable truncated conical shells reinforced by FGM stiffeners[J]. *Mechanics of Composite Materials*, 2019, **54**(6): 745-764.
- [7] 曹志远. 不同条件功能梯度矩形板固有频率解的一般表达式[J]. 复合材料学报, 2005, **22**(5): 172-177. (CAO Zhiyuan. Unified expression of natural frequency solutions for functionally graded composite rectangular plates under various boundary conditions[J]. *Acta Materiae Compositae Sinica*, 2005, **22**(5): 172-177. (in Chinese))
- [8] TU T M, QUOC T H, VAN-LONG N. Vibration analysis of functionally graded plates using the eight-unknown higher order shear deformation theory in thermal environments[J]. *Aerospace Science and Technology*, 2018, **84**(5): 698-711.
- [9] HU Y D, ZHANG Z Q. The bifurcation analysis on the circular functionally graded plate with combination resonances[J]. *Nonlinear Dynamics*, 2012, **67**(3): 1779-1790.
- [10] ZHANG W, HAO Y X, YANG J. Nonlinear dynamics of FGM circular cylindrical shell with clamped-clamped edges[J]. *Composite Structures*, 2012, **94**(3): 1075-1086.
- [11] AN F X, CHEN F Q. Multi-pulse chaotic motions of functionally graded truncated conical shell under complex loads[J]. *Nonlinear Dynamics*, 2017, **89**(3): 1753-1778.
- [12] SAHU N K, BISWAL D K, JOSEPH S V, et al. Vibration and damping analysis of doubly curved viscoelastic-FGM sandwich shell structures using FOSDT[J]. *Structures*, 2020, **26**: 24-38.
- [13] LI X, DU C C, LI Y H. Parametric resonance of a FG cylindrical thin shell with periodic rotating angular speeds in thermal environment[J]. *Applied Mathematical Modelling*, 2018, **59**(7): 393-409.
- [14] ZHANG D G, ZHOU Y H. A theoretical analysis of FGM thin plates based on physical neutral surface[J]. *Computational Materials Science*, 2008, **44**(2): 716-720.
- [15] ZHANG D G. Nonlinear bending analysis of FGM beams based on physical neutral surface and high order shear deformation theory[J]. *Composite Structure*, 2013, **100**: 121-126.
- [16] ZHANG D G. Nonlinear static analysis of FGM infinite cylindrical shallow shells based on physical neutral surface and high order shear deformation theory[J]. *Applied Mathematical Modelling*, 2015, **39**(5/6): 1587-1596.
- [17] MIYA K, HARA K, SOMEYA K. Experimental and theoretical study on magnetoelastic buckling of a ferromagnetic cantilevered beam-plate[J]. *Journal of Applied Mechanics*, 1978, **45**(2): 355-360.
- [18] 刘旭, 姚林泉. 热环境中旋转功能梯度纳米环板的振动分析[J]. 应用数学和力学, 2020, **41**(11): 1224-1236. (LIU Xu, YAO Linqun. Vibration analysis of rotating functionally gradient nano annular plates in thermal environment[J]. *Applied Mathematics and Mechanics*, 2020, **41**(11): 1224-1236. (in Chinese))
- [19] 陈明飞, 刘坤鹏, 靳国永, 等. 面内功能梯度三角形板等几何面内振动分析[J]. 应用数学和力学, 2020, **41**(2): 156-170. (CHEN Mingfei, LIU Kumpeng, JIN Guoyong, et al. Isogeometric in-plane vibration analysis of functionally graded triangular plates[J]. *Applied Mathematics and Mechanics*, 2020, **41**(2): 156-170. (in Chinese))
- [20] WANG X Z, LEE J S, ZHENG X J. Magneto-thermo-elastic instability of ferromagnetic plates in thermal and magnetic fields[J]. *International Journal of Solids and Structures*, 2003, **40**(22): 6125-6142.
- [21] MOHAJERANI S A, MOHAMMADZADEH A, NIKKHAH-BAHRAMI M N. An exact solution for vibration analysis of soft ferromagnetic rectangular plates under the influence of magnetic field with levy type boundary conditions[J]. *Journal of Solid Mechanics*, 2017, **9**(1): 186-197.
- [22] 胡宇达, 张金志. 轴向运动载流导电板磁热弹性耦合动力学方程[J]. 力学学报, 2013, **45**(5): 792-796. (HU Yuda, ZHANG Jinzhi. Magneto-thermo-elastic coupled dynamics equations of axially moving carry current plate in magnetic field[J]. *Chinese Journal of Theoretical and Applied Mechanics*, 2013, **45**(5): 792-796. (in Chinese))
- [23] HU Y D, CAO T X, XIE M X. Magnetic-structure coupling dynamic model of a ferromagnetic plate parallel

- moving in air-gap magnetic field[J]. *Acta Mechanica Sinica*, 2022, **38**(10): 522084.
- [24] 胡宇达, 刘超. 线载和弹性支承作用面内运动薄板磁固耦合双重共振[J]. 应用数学和力学, 2021, **42**(7): 713-722. (HU Yuda, LIU Chao. Double resonance of magnetism-solid coupling of in-plane moving thin plates with linear loads and elastic supports[J]. *Applied Mathematics and Mechanics*, 2021, **42**(7): 713-722. (in Chinese))
- [25] 沈璐璐, 蔡方圆, 杨博. 功能梯度压电板柱面弯曲的弹性力学解[J]. 应用数学和力学, 2023, **44**(3): 272-281. (SHEN Lulu, CAI Fangyuan, YANG Bo. Elasticity solutions for cylindrical bending of functionally graded piezoelectric material plates[J]. *Applied Mathematics and Mechanics*, 2023, **44**(3): 272-281. (in Chinese))
- [26] MIKILYANA M, MARZOCCA P. Dynamic instability of electroconductive cylindrical shell in a magnetic field[J]. *International Journal of Solids and Structures*, 2019, **160**: 168-176.
- [27] MOLCHENKO L V, LOOS I I, VASILEVA L Y, et al. Magnetoelastic deformation of isotropic variable-stiffness shells of revolution: allowing for joule heat and geometrical nonlinearity[J]. *International Applied Mechanics*, 2020, **56**(2): 198-207.
- [28] LI Z, WANG Q S, QIN B, et al. Vibration and acoustic radiation of magneto-electro-thermo-elastic functionally graded porous plates in the multi-physics fields[J]. *International Journal of Mechanical Sciences*, 2020, **185**(11): 105850.
- [29] MEHDITABAR A, RAHIMI G H, ANSARI-SADRABADI S. Three-dimensional magneto-thermo-elastic analysis of functionally graded cylindrical shell[J]. *Applied Mathematics and Mechanics(English Edition)*, 2017, **38**(4): 479-494.
- [30] LIU Y F, QIN Z Y, CHU F L. Nonlinear forced vibrations of functionally graded piezoelectric cylindrical shells under electric-thermo-mechanical loads[J]. *International Journal of Mechanical Sciences*, 2021, **201**: 106474.
- [31] DU C C, LI Y H. Nonlinear resonance behavior of functionally graded cylindrical shells in thermal environments[J]. *Composite Structures*, 2013, **102**(8): 164-174.
- [32] ZHANG D G, ZHOU Y H. A theoretical analysis of FGM thin plates based on physical neutral surface[J]. *Computational Materials Science*, 2009, **44**(2): 716-720.
- [33] 梁斌, 项爽, 李戎, 等. 旋转功能梯度圆柱壳振动影响因素研究[J]. 船舶力学, 2013, **17**(12): 1460-1472. (LIANG Bin, XIANG Shuang, LI Rong, et al. Study of effective factors for the vibration of rotating functionally graded cylindrical shells[J]. *Journal of Ship Mechanics*, 2013, **17**(12): 1460-1472. (in Chinese))
- [34] SHEN H S. Nonlinear vibration of shear deformable FGM cylindrical shells surrounded by an elastic medium[J]. *Composite Structures*, 2012, **94**(3): 1144-1154.
- [35] LOY C T, LAM K Y, REDDY J N. Vibration of functionally graded cylindrical shells[J]. *International Journal of Mechanical Sciences*, 1999, **41**(3): 309-324.